

This is a self-archived version of an original article. This version may differ from the original in pagination and typographic details.

Author(s): Matus, María Francisca; Häkkinen, Hannu

Title: Atomically Precise Gold Nanoclusters : Towards an Optimal Biocompatible System from a Theoretical–Experimental Strategy

Year: 2021

Version: Accepted version (Final draft)

Copyright: © 2021 Wiley-VCH GmbH

Rights: In Copyright

Rights url: <http://rightsstatements.org/page/InC/1.0/?language=en>

Please cite the original version:

Matus, M. F., & Häkkinen, H. (2021). Atomically Precise Gold Nanoclusters : Towards an Optimal Biocompatible System from a Theoretical–Experimental Strategy. *Small*, 17(27), Article 2005499. <https://doi.org/10.1002/sml.202005499>

1
2
3
4 **Atomically Precise Gold Nanoclusters: Towards an Optimal Biocompatible System**
5
6 **from a Theoretical–Experimental Strategy**
7

8
9
10 *María Francisca Matus and Hannu Häkkinen**
11

12
13
14
15 Dr. M.F. Matus

16 Department of Physics, Nanoscience Center (NSC)

17 University of Jyväskylä

18 FI-40014 Jyväskylä, Finland
19
20
21

22
23
24 Prof. Dr. H. Häkkinen

25 Departments of Physics and Chemistry, Nanoscience Center (NSC)

26 University of Jyväskylä

27 FI-40014 Jyväskylä, Finland
28
29

30 E-mail: hannu.j.hakkinen@jyu.fi
31
32
33
34
35
36

37 **Keywords**
38

39
40 Gold Nanoclusters, Biomedical Applications, Nanomedicine, Biocompatibility, Atomistic
41 Simulations
42
43
44
45
46
47

48
49 Potential biomedical applications of gold nanoparticles have increasingly been reported with
50 great promise for diagnosis and therapy of several diseases. However, for such a versatile
51 nanomaterial, the advantages and potential health risks need to be addressed carefully, as the
52 available information about their toxicity is limited and inconsistent. Atomically precise gold
53 nanoclusters (AuNCs) have emerged to overcome this challenge due to their unique features,
54
55
56
57
58
59
60
61
62
63
64
65

1
2
3
4 such as superior stability, excellent biocompatibility, and efficient renal clearance.
5
6 Remarkably, the elucidation of their structural and physicochemical properties provided by
7
8 theory–experiment investigations offers exciting opportunities for site-specific bio-
9
10 functionalization of the nanoparticle surface, which remains a significant concern for most
11
12 of the materials in the biomedical field. This Concept highlights the advantages conferred by
13
14 atomically precise AuNCs for biomedical applications and the powerful strategy combining
15
16 computational and experimental studies towards finding an optimal biocompatible AuNC-
17
18 based nanosystem.
19
20
21
22
23
24
25
26

27 **1. Introduction**

28
29 Gold nanoparticles (AuNPs) are one of the most exploited nanomaterials in different fields
30
31 of science,^[1–3] attracting special interest in biomedicine.^[4,5] Over the past decade, diverse
32
33 applications of AuNPs have been mainly focused on drug delivery, imaging techniques, and
34
35 photothermal therapy.^[6] Their high versatility has enabled them to show promise in diagnosis
36
37 and therapy for several diseases, such as cancers, hepatitis, tuberculosis, and Alzheimer’s
38
39 disease.^[7] However, despite the extensive *in vitro* and *in vivo* studies demonstrating the
40
41 efficacy of a large variety of AuNPs, the *in vivo* toxicity remains a significant problem,
42
43 directly related to their size and aggregation.^[8,9] Either their large size (typically above 50
44
45 nm) or the eventual formation of large aggregates (around 20–100 nm) means that the AuNPs
46
47 cannot be metabolized^[10] and are unable to escape the reticuloendothelial system (RES), with
48
49 the consequent accumulation in some organs, like liver and spleen.^[7] Therefore, with the
50
51 increasing progress of bio-applications, it becomes critical to evaluate the toxicity and
52
53 biocompatibility, which particularly in the case of AuNPs, is still contradictory.^[3]
54
55
56
57
58
59
60
61
62
63
64
65

1
2
3
4
5
6
7 In the past 10+ years, a singular type of ultra-small AuNPs, so-called gold nanoclusters
8 (AuNCs), has emerged.^[11,12] Unlike colloidal and polydisperse gold nanoparticles, AuNCs
9
10 are composed of a few to some hundreds of gold atoms, which corresponds to NPs smaller
11
12 than 2 nm metal core diameter with a uniform crystal structure. AuNCs are unique since their
13
14 structures can be determined to atomic precision by using single crystal X-ray diffraction
15
16 methods.^[11,13,14] This fact has enabled accurate studies of their physicochemical properties,
17
18 highlighting their atomically precise structure that can bring much more control for binding
19
20 selectivity, offering a higher precision in the exploration of their potential applications, than
21
22 what can be achieved with the colloidal noble metal NPs. In biomedicine, they have gained
23
24 growing interest due to their extraordinary properties such as facile synthesis, superior
25
26 stability, excellent biocompatibility and efficient renal clearance.^[14,15]
27
28
29
30
31
32
33
34
35
36
37

38 Functionalization of their surface takes the AuNCs to the next level allowing them to exert
39
40 their action at a specific site. However, it also creates one of the main challenges because the
41
42 chemical and physical properties of AuNCs can be significantly affected by their surface
43
44 modification.^[16] Functionalization also increases the system's complexity due to the high
45
46 number of atomic and molecular interactions involved, which, together with its small size,
47
48 hinder its development at the experimental level. This is where the use of computational
49
50 modeling begins to become particularly important. Computational tools provide useful
51
52 approaches to addressing several challenges in the design of nanosystems, including the need
53
54 for a better understanding of nanoparticle behavior and the prediction of different
55
56 physicochemical properties at the atomic level. The advances in the field of thiolate-protected
57
58
59
60
61
62
63
64
65

1
2
3
4 AuNCs have been powered by this close interaction of experimental and theoretical studies.
5
6 To date, several precise structures have been revealed either by X-ray diffraction or
7
8 theoretically predicted by employing density functional theory (DFT) computation.^[17]
9
10 Combination of theory and experiment has permitted the elucidation of several properties,
11
12 including electronic structures, luminescence, optical absorption, as well as the structural
13
14 patterns of their high symmetric cores and their protecting ligand motifs.^[17,18] This well-
15
16 defined structural information offers a particularly attractive chance for a better
17
18 understanding of the structure–property relationships of these intriguing systems and the
19
20 unique opportunity for highly-controlled adjustments of specific features in order to increase
21
22 the desired properties in different applications.
23
24
25
26
27
28
29
30
31

32 This Concept focuses specifically on the advantages conferred by atomically precise AuNCs
33
34 for biomedical applications and the powerful strategic approach of using theory and
35
36 experiment in a complementary manner towards finding an optimal biocompatible AuNC-
37
38 based nanosystem.
39
40
41
42
43
44

45 **2. The Unique Properties of Ultra-small AuNCs for Biomedical Applications**

46
47
48 Potential biomedical applications of any nanosystem are mainly linked to some critical
49
50 factors, such as size, physicochemical properties and surface chemistry.^[19] AuNCs possess a
51
52 unique combination of these features, which makes them particularly promising in the field
53
54 of biomedicine. Their ultra-small size favors the renal clearance^[20,21] and helps them evade
55
56 the uptake by the RES.^[22] Likewise, their small size and the benefit from the enhanced
57
58
59
60
61
62
63
64
65

1
2
3
4 permeability and retention (EPR)^[23] and nanomaterials-induced endothelial cell leakiness
5
6 (NanoEL)^[24] effects allow exceptional tumor accumulation properties.
7
8
9

10
11 Highly stable optical properties are another advantage. AuNCs display molecular-like
12
13 properties such as discrete electronic transitions, leading to photoluminescence (PL)
14
15 properties tunable from the ultra-violet (UV) to near-infrared (NIR) region,^[25,26] which offers
16
17 great potential for their detection *in vivo* by multimodal imaging techniques with excellent
18
19 performance, overcoming difficulties related to PL quenching of larger plasmonic AuNPs.^[15]
20
21
22
23
24
25
26
27

28
29 Proper surface functionalization is also critical for the biocompatibility of the nanosystem.
30
31 The surface ligands significantly influence the solubility, stability, and determine the
32
33 interactions of the nanomaterial with the environment.^[27] The biocompatibility of the AuNCs
34
35 can be further improved by taking advantage of their facile surface modification. Several
36
37 efficient strategies have been developed to synthesize AuNCs protected by thiolate ligands
38
39 with atomic precision,^[14] resulting in water-soluble AuNCs, which are especially desired in
40
41 applications for biological systems. Atomically precise AuNCs functionalized with other
42
43 biocompatible molecules offer unique opportunities in theranostics, allowing more control
44
45 over such sensitive and challenging issues as protein corona formation, *in vivo*
46
47 biodistribution, and cellular uptake efficiency, to name a few.^[28] Considering this huge
48
49 potential within the field of nanomedicine, investigations using atomically precise, water-
50
51 soluble, and monodisperse AuNCs, need to be emphasized.
52
53
54
55
56
57
58
59
60
61
62
63
64
65

1
2
3
4 In radiotherapy, which is one of the leading types of cancer treatment, AuNCs with
5
6 atomically precise structure provide a remarkable opportunity for radiosensitizer
7
8 investigations (Figure 1). Beyond just showing enhancement of the radiotherapeutic activity,
9
10 they allow to accurately associate radiosensitizer properties with the inner core structure and
11
12 ligands.^[29] For instance, Xie group (2014 and 2015) has developed and studied *in vivo* a
13
14 series of sub-2 nm glutathione (GSH)-protected AuNCs with these features, such as Au₁₀₋₁₂(GSH)₁₀₋₁₂,^[30]
15
16 Au₂₅(GSH)₁₈,^[31] and Au₂₉₋₄₃(GSH)₂₇₋₃₇.^[32] NCs, which showed a ultrahigh
17
18 tumor uptake and low toxicity. They found that the AuNCs could readily escape from the
19
20 RES and accumulate in tumors *via* the improved EPR effect, leading to enhanced cancer
21
22 radiotherapy. In 2019, Jia and coworkers reported a structurally defined
23
24 alkynyl(levonorgestrel)-protected Au₈ NC as an effective and biocompatible radiosensitizer
25
26 that causes irreversible apoptosis of tumor cells due to their localized production of reactive
27
28 oxygen species (ROS).^[29] *In vivo* models showed a significant inhibition rate of 74.2 % when
29
30 tumors are treated with Au₈(levonorgestrel)₈ NCs and an X-ray dose of 4 Gray (Gy)
31
32 compared to tumors irradiated with X-ray alone. Recently, targeting capacity of
33
34 radiosensitizers for prostate cancer cells has also been reported with promising results. Luo
35
36 *et al.* (2019) designed Au₂₅ NCs protected with a peptide-tagged prostate specific membrane
37
38 antigen targeting ligand (CY-PSMA-1) with the ability to target PSMA receptor positive
39
40 cancer cells (PC3pip).^[33] The results demonstrated a significantly enhanced tumor-
41
42 suppressing efficacy of the Au₂₅S_(18-m)(CY-PSMA-1)_m (m=0–18) NCs *in vivo* when combined
43
44 with X-ray irradiation (6 Gy) and showed fast renal clearance from the mice body.
45
46
47
48
49
50
51
52
53
54
55
56

57 Targeting strategies in AuNCs with atomic precise structures has expanded well beyond the
58
59 cancer nanomedicine field. For example, by replacing GSH ligands with (4-
60
61
62
63
64
65

1
2
3
4 mercaptobutyl)triphenyl-phosphonium bromide (MTPB) on fluorescent Au₁₈(GSH)₁₄ NCs
5
6 through a ligand exchange method, mitochondrial targeting was achieved.^[34] While the
7
8 unmodified Au₁₈(GSH)₁₄ preferably accumulated in lysosomes, the resulting water-soluble
9
10 Au₁₈(GSH)₁₂(MTPB)₂ NCs showed higher accumulation at the mitochondrial site with their
11
12 initial optical properties largely unaffected. Due to the central role of mitochondria in critical
13
14 cellular processes such as metabolism and apoptosis, this approach is highly attractive to
15
16 stimulate extensive studies and potential applications for diagnosis and treatment of several
17
18 diseases, such as diabetes, obesity, neurodegenerative diseases, and cancers^[35] at the cell and
19
20 organelle levels.
21
22
23
24
25
26
27
28
29
30

31 Another growing global threat is antibiotic resistance.^[36] Thus, alternatives to conventional
32
33 antibiotics that address bacterial infections are highly desirable. For several years, the NP
34
35 activity against multidrug-resistant pathogens has been demonstrated.^[37,38] However,
36
37 potential antimicrobial activity of AuNPs reduced to the NC range remained practically
38
39 unexplored until 2017 when Zheng and colleagues studied the antibacterial potential of 6-
40
41 mercaptohexanoic acid (MHA)-protected Au₂₅ NCs on both Gram-positive and Gram-
42
43 negative strains.^[39] Au₂₅(MHA)₁₈ NCs showed a high wide-spectrum antimicrobial activity,
44
45 killing more than 90 % of Gram-positive (*Staphylococcus aureus*, *Staphylococcus epidermis*,
46
47 and *Bacillus subtilis*) and Gram-negative bacteria (*Escherichia coli* and *Pseudomonas*
48
49 *aeruginosa*) with a dose of 0.1 mM. They found that Au₂₅(MHA)₁₈ NCs could induce a
50
51 metabolic imbalance in the cells, leading to a significant increase of intracellular ROS
52
53 production, which confers the bacteria-killing effect. In sharp contrast, the observed
54
55 antimicrobial effect is absent in the AuNPs counterparts protected with the same ligand. This
56
57
58
59
60
61
62
63
64
65

1
2
3
4 study provides a proof of principle for the utilization of AuNCs as an alternative wide-
5
6 spectrum antimicrobial agent and, at the same time, with potential high biocompatibility in
7
8 the host human cells due to the noble qualities of gold^[40,41] (Figure 1). Even more interesting,
9
10 AuNCs possess higher structural stability than silver (Ag) NPs and AgNCs,^[42] which have
11
12 led the investigations in this field due to the intrinsic antimicrobial capacity of Ag.^[43] Hence,
13
14 AuNCs could be one of the best candidates for the development of a new generation of
15
16 antimicrobial agents.
17
18
19
20
21
22

23
24 The outstanding role of atomistically well-defined monodisperse AuNCs as contrast agents
25
26 in biological imaging applications has also been demonstrated through site-specific
27
28 conjugation to biomolecules^[44,45] (Figure 1). AuNCs would allow addressing some
29
30 fundamental challenges in this field, such as the long-term stability of markers and their
31
32 biocompatibility for clinical applications,^[46] offering distinctive features to the development
33
34 of more direct and robust tracking strategies *in vitro* and *in vivo*. In 2014, Marjomäki *et al.*
35
36 reported a site-specific covalent conjugation of water-soluble *para*-mercaptobenzoic acid
37
38 (*p*MBA)-protected Au₁₀₂ NCs, functionalized by a thiol-reactive linker (*N*-(6-
39
40 hydroxyhexyl)maleimide) to target cysteine sites of capsid proteins in echovirus 1 (EV1) and
41
42 Coxsackievirus B3 (CVB3) without compromising their infectivity.^[44] The well-defined
43
44 structures of both maleimide functionalized-Au₁₀₂(*p*MBA)₄₄ NCs and viruses capsid allowed
45
46 analyzing the specific spatial ordering of enterovirus–cluster conjugates in both virus types
47
48 through transmission electron microscopy (TEM). One year later and taking advantage of
49
50 this strategy, Au₁₀₂(*p*MBA)₄₄ NCs were utilized for noncovalent linking to the capsid of EV1
51
52 and CVA9 enteroviruses.^[45] AuNCs were conjugated to a Pleconaril drug-like molecule,
53
54 which was used to target site-specifically the hydrophobic pocket of the virus capsid,
55
56
57
58
59
60
61
62
63
64
65

1
2
3
4 enabling the visualization of the viruses *via* TEM while retaining their infectivity. These
5
6 approaches may be extended not only for structural studies of viral uncoating, but also for
7
8 revealing more fundamentals of virus and other biomolecules entry pathways into cells. In
9
10 this context, a AuNC-labeled fibroblast growth factor 21 (FGF21) tracking technique was
11
12 reported in human primary adipocytes.^[47] By using *meta*-mercaptobenzoic acid (3MBA)-
13
14 protected Au₁₄₄ NCs conjugated with FGF21 and cryo-electron tomography (cryo-ET),
15
16 Azubel and coworkers (2019) were able to capture different states of activation,
17
18 internalization, and traffic of the FGF21/FGFR1c/β-Klotho (FGF-receptor-cofactor)
19
20 complex demonstrating its clathrin-dependent pathway endocytosis.^[47] The paired or
21
22 unpaired FGF21 functionalized-Au₁₄₄(3MBA)₋₄₀ NCs distribution in different vesicular
23
24 compartments helped to confirm the overall 2:2:2 stoichiometry of the ternary complex in
25
26 the human fat cells and observe its disruption at specific levels in the pathway. This is the
27
28 first study in which, through Au₁₄₄(3MBA)₋₄₀ NCs labeling, a three-dimensional picture of
29
30 the entire endocytosis pathway is achieved.

31
32
33 The photoluminescence of AuNCs is another significant feature that makes them a promising
34
35 agent for biological imaging and medical diagnosis.^[48] In a recent study, Liu *et al.* (2019)
36
37 demonstrated the potential of water-soluble Au₂₅(GSH)₁₈ NCs as an efficient near-infrared II
38
39 (NIR-II) fluorophore in *in vivo* models.^[49] Au₂₅(GSH)₁₈ NCs can emit fluorescence at 1100–
40
41 1350 nm and showed unique features of particular relevance for biological and clinical
42
43 applications, such as high quantum yield (QY) that can be further increased by metal-atom
44
45 doping, and efficient renal clearance even at an ultrahigh dose of 100 mg kg⁻¹. It is noteworthy
46
47 that most of the nanomaterials (inorganic and organic) that have shown promising features
48
49 as agents for bioimaging meet only one of these requirements.^[49] Thus, it is time to expand
50
51 the investigations of AuNCs-based agents in this field, but now including comparisons with
52
53
54
55
56
57
58
59
60
61
62
63
64
65

1
2
3
4 more promising and emerging nanostructures, such as palladium (Pd)-based
5
6 nanomaterials.^[50] Interestingly, Pd nanosheets (16 nm) were reported to have high
7
8 photothermal efficiency and showed superior stability, measured against AuNPs
9
10 (nanorods).^[51] However, these findings might substantively differ when the point of
11
12 comparison is AuNCs instead, due to their exceptional features described above, which can
13
14 only be obtained when the size of NPs is reduced to the NC range.
15
16
17
18
19
20
21
22

23 **3. Manipulation of the System at Atomic Level: In Pursuit of the Most Realistic** 24 25 **Theoretical Model** 26

27
28
29 Clearly, the extraordinary properties that atomically precise AuNCs have exhibited in
30
31 experimental research, place them as one of the most promising nanomaterials within the
32
33 field of biomedicine. However, in order to extend their applications and achieve their clinical
34
35 translation, some current fundamental challenges need to be considered and understood in
36
37 more detail, such as improving the PL quantum yield, increasing the yield of the synthesis,
38
39 and precisely controlling the surface modification.^[16] To achieve this purpose, an
40
41 interdisciplinary strategy becomes critical. The use of theoretical models either as a
42
43 predictive tool or as complementary to experimental work could provide crucial information
44
45 for the design of optimal AuNC-based biocompatible systems, including their geometric
46
47 structure, electronic structure, reaction mechanisms, structure–activity relationship as well as
48
49 the effects of the surrounding environment (**Figure 2**).
50
51
52
53
54
55
56
57
58
59
60
61
62
63
64
65

1
2
3
4 DFT calculations have been extensively used and synergistically combined with experiments
5
6 for AuNCs characterization, showing an outstanding performance in their structure and
7
8 properties elucidation.^[52] By this method, some aspects like general structures, core-shell
9
10 geometries, and isomerization mechanisms of diverse atomically precise AuNCs have been
11
12 predicted with high accuracy.^[17,53,54] Furthermore, DFT has supported the development of a
13
14 molecular mechanics force field for thiolate-protected AuNCs compatible with the well-
15
16 known biomolecular force field AMBER.^[55] This allows investigating the dynamics of the
17
18 AuNCs in a more realistic biological environment (i.e., including solvent, counterions) by
19
20 employing classical molecular dynamics (MD) simulations. Combined with the existing
21
22 biomolecular force fields in AMBER, interactions between the gold clusters and
23
24 biomolecules, such as proteins, cell membranes, or nucleic acids can be explored in long time
25
26 scales (in principle, from hundreds of nanoseconds to microsecond by using supercomputers)
27
28 with an all-atom description. The precise atomic structure of AuNCs is crucial in the
29
30 construction of these theoretical models and particularly relevant for investigations of the
31
32 bio–nano interface and addressing the challenge of protein corona formation in an exhaustive
33
34 way. Correlation of these theoretical predictions with experimental data from methods like
35
36 X-ray diffraction and Ultraviolet-visible (UV-vis) spectroscopy offers the possibility to
37
38 determine which features of the AuNC can be adapted to increase the desired properties.
39
40
41
42
43
44
45
46
47
48
49
50

51 Thiolate-for-thiolate ligand exchange reaction is a well-established technique and widely
52
53 used for surface modification of monolayer-protected AuNCs.^[56–58] Although this strategy
54
55 had been utilized for many years since its origin, it was not until 2012 when Heinecke and
56
57 colleagues reported the structural basis of this strategy by employing a computational-
58
59
60
61
62
63
64
65

1
2
3
4 experimental approach.^[59] They used *p*-bromobenzene thiol (*p*BBT) as the incoming ligand
5
6 and performed the exchange reaction to obtain the first single-crystal X-ray structure of a
7
8 partially exchanged $\text{Au}_{102}(\text{pMBA})_{40}(\text{pBBT})_4 \text{ NC}$. They studied the regioselectivity of the
9
10 reaction based on the 22 symmetry-unique *p*MBA ligand sites of $\text{Au}_{102}(\text{pMBA})_{44}$ and
11
12 postulated the mechanistic pathway for the reaction by DFT calculations. Ligand place-
13
14 exchange was exhibited in 2 of the 22 symmetrically unique ligand sites, each of them bonded
15
16 to a different solvent-exposed gold atom. Together with a complete reaction path modeling
17
18 both thiol and thiolate incoming ligands by DFT, the authors suggested an associative
19
20 exchange mechanism. Following the same line, Rojas-Cervellera *et al.* (2017) studied the
21
22 molecular mechanism of ligand exchange reaction involving AuNCs and proteins by
23
24 combining classical and *ab initio* quantum mechanics/molecular mechanics (QM/MM) MD
25
26 simulations.^[60] Inspired by the experimental work of Ackerson group (2006), they modeled
27
28 the conjugation of $\text{Au}_{25}(\text{GSH})_{18}^- \text{ NC}$ with a single chain Fv (scFv) fragment of the NC10
29
30 antibody in water in order to obtain an atomistic description of this reaction.^[61] Two
31
32 particular sites in the Au_{25} V-shaped staple were considered (side thiolate and apex thiolate)
33
34 and thus, two different routes were explored to determine which one is more readily
35
36 exchanged. Calculations showed that the reaction follows an associative $\text{S}_{\text{N}}2$ -like reaction
37
38 mechanism and the substitution of the side ligand is favored over the apex one, which
39
40 interestingly, is in high accordance with the study described above using
41
42 $\text{Au}_{102}(\text{pMBA})_{40}(\text{pBBT})_4 \text{ NCs}$.^[59] The results also suggested that the presence of positively
43
44 charged residues surrounding the incoming ligand facilitates the adsorption of the protein on
45
46 the AuNC surface. These approaches are attractive for site-selective modification of AuNCs
47
48 displaying desired properties for stable and functional AuNC-biomolecule conjugates.
49
50
51
52
53
54
55
56
57
58
59
60
61
62
63
64
65

1
2
3
4 In 2016, Salorinne *et al.* reported a complete ^1H and ^{13}C nuclear magnetic resonance (NMR)
5
6 chemical shifts assignment for all ligands of the atomically precise $\text{Au}_{102}(\text{pMBA})_{44}$ NC in
7
8 water by employing a combination of multidimensional NMR methods, DFT calculations,
9
10 and MD simulations.^[62] By using these computational techniques, it was possible to obtain a
11
12 precise structural and dynamical information of the ligand shell and correlate it with ligand
13
14 symmetry environments observed in the single-crystal X-ray structure.^[63] This study is
15
16 particularly attractive for accurate functionalization strategies and gives the potential to
17
18 control and understand in more detail the bio–nano interface and the transformations that
19
20 AuNCs undergo in the biological environment.
21
22
23
24
25
26
27
28

29 Another interdisciplinary study was carried out in 2017, where the atomic structure and
30
31 dynamics of the ligand layer of $\text{Au}_{68}(\text{3MBA})_{\sim 32}$ and $\text{Au}_{144}(\text{3MBA})_{\sim 40}$ NCs was revealed.^[64]
32
33 By a combination of MD simulations and DFT calculations, and supported by NMR, UV-vis
34
35 absorption, and Infrared (IR) spectroscopy the authors suggested a distinct chemistry in the
36
37 ligand–metal interface, which is absent in other known thiol-stabilized AuNCs. Interestingly,
38
39 they found weak π –Au and $\text{O}=\text{C}-\text{OH}\cdots\text{Au}$ interactions protecting the metal core in addition
40
41 to the covalent S–Au bond formation. This finding could support some particular features
42
43 observed previously in 3MBA-protected AuNCs, such as their reactivity to thiol-modified
44
45 DNA and proteins^[65] and the unusually low ligand coverage in the $\text{Au}_{144}(\text{3MBA})_{\sim 40}$ NC.^[66]
46
47
48
49 In addition to explaining or validating experimental evidence, this finding offers new
50
51 possibilities for the development of novel hybrid nanosystems based on 3MBA-protected
52
53 AuNCs (e.g., as drug delivery systems, biosensors) and understand their functionalization
54
55
56
57
58
59
60
61
62
63
64
65
66
67
68
69
70
71
72
73
74
75
76
77
78
79
80
81
82
83
84
85
86
87
88
89
90
91
92
93
94
95
96
97
98
99
100
101
102
103
104
105
106
107
108
109
110
111
112
113
114
115
116
117
118
119
120
121
122
123
124
125
126
127
128
129
130
131
132
133
134
135
136
137
138
139
140
141
142
143
144
145
146
147
148
149
150
151
152
153
154
155
156
157
158
159
160
161
162
163
164
165
166
167
168
169
170
171
172
173
174
175
176
177
178
179
180
181
182
183
184
185
186
187
188
189
190
191
192
193
194
195
196
197
198
199
200
201
202
203
204
205
206
207
208
209
210
211
212
213
214
215
216
217
218
219
220
221
222
223
224
225
226
227
228
229
230
231
232
233
234
235
236
237
238
239
240
241
242
243
244
245
246
247
248
249
250
251
252
253
254
255
256
257
258
259
260
261
262
263
264
265
266
267
268
269
270
271
272
273
274
275
276
277
278
279
280
281
282
283
284
285
286
287
288
289
290
291
292
293
294
295
296
297
298
299
300
301
302
303
304
305
306
307
308
309
310
311
312
313
314
315
316
317
318
319
320
321
322
323
324
325
326
327
328
329
330
331
332
333
334
335
336
337
338
339
340
341
342
343
344
345
346
347
348
349
350
351
352
353
354
355
356
357
358
359
360
361
362
363
364
365
366
367
368
369
370
371
372
373
374
375
376
377
378
379
380
381
382
383
384
385
386
387
388
389
390
391
392
393
394
395
396
397
398
399
400
401
402
403
404
405
406
407
408
409
410
411
412
413
414
415
416
417
418
419
420
421
422
423
424
425
426
427
428
429
430
431
432
433
434
435
436
437
438
439
440
441
442
443
444
445
446
447
448
449
450
451
452
453
454
455
456
457
458
459
460
461
462
463
464
465
466
467
468
469
470
471
472
473
474
475
476
477
478
479
480
481
482
483
484
485
486
487
488
489
490
491
492
493
494
495
496
497
498
499
500
501
502
503
504
505
506
507
508
509
510
511
512
513
514
515
516
517
518
519
520
521
522
523
524
525
526
527
528
529
530
531
532
533
534
535
536
537
538
539
540
541
542
543
544
545
546
547
548
549
550
551
552
553
554
555
556
557
558
559
560
561
562
563
564
565
566
567
568
569
570
571
572
573
574
575
576
577
578
579
580
581
582
583
584
585
586
587
588
589
590
591
592
593
594
595
596
597
598
599
600
601
602
603
604
605
606
607
608
609
610
611
612
613
614
615
616
617
618
619
620
621
622
623
624
625
626
627
628
629
630
631
632
633
634
635
636
637
638
639
640
641
642
643
644
645
646
647
648
649
650
651
652
653
654
655
656
657
658
659
660
661
662
663
664
665
666
667
668
669
670
671
672
673
674
675
676
677
678
679
680
681
682
683
684
685
686
687
688
689
690
691
692
693
694
695
696
697
698
699
700
701
702
703
704
705
706
707
708
709
710
711
712
713
714
715
716
717
718
719
720
721
722
723
724
725
726
727
728
729
730
731
732
733
734
735
736
737
738
739
740
741
742
743
744
745
746
747
748
749
750
751
752
753
754
755
756
757
758
759
760
761
762
763
764
765
766
767
768
769
770
771
772
773
774
775
776
777
778
779
780
781
782
783
784
785
786
787
788
789
790
791
792
793
794
795
796
797
798
799
800
801
802
803
804
805
806
807
808
809
810
811
812
813
814
815
816
817
818
819
820
821
822
823
824
825
826
827
828
829
830
831
832
833
834
835
836
837
838
839
840
841
842
843
844
845
846
847
848
849
850
851
852
853
854
855
856
857
858
859
860
861
862
863
864
865
866
867
868
869
870
871
872
873
874
875
876
877
878
879
880
881
882
883
884
885
886
887
888
889
890
891
892
893
894
895
896
897
898
899
900
901
902
903
904
905
906
907
908
909
910
911
912
913
914
915
916
917
918
919
920
921
922
923
924
925
926
927
928
929
930
931
932
933
934
935
936
937
938
939
940
941
942
943
944
945
946
947
948
949
950
951
952
953
954
955
956
957
958
959
960
961
962
963
964
965
966
967
968
969
970
971
972
973
974
975
976
977
978
979
980
981
982
983
984
985
986
987
988
989
990
991
992
993
994
995
996
997
998
999
1000

1
2
3
4
5
6
7 Motivated by the ability of AuNCs as biocompatible contrast agents in virus imaging
8 demonstrated experimentally and described in the previous section,^[45] Pohjolainen and
9 coworkers (2017) performed a series of all-atom MD simulations combined with non-
10 equilibrium free energy calculations to study in detail the effect of $\text{Au}_{102}(\text{pMBA})_{44}$ NCs on
11 the binding affinity of the AuNC-linked pocket factor–virus complex.^[67] Half- and fully
12 deprotonated states of *p*MBA ligand layer were considered and included in a complete system
13 containing the full EV1 virus and the hydrophobic pocket factors in water, making it able to
14 obtain molecule-scale structural information and complement the experimental findings.
15 They found that the binding affinity of AuNC-linked pocket factor–virus is pH-sensitive.
16 Specifically, the affinity of this complex (before AuNC labeling) is unaffected when fully
17 deprotonated $\text{Au}_{102}(\text{pMBA})_{44}$ NCs are conjugated to the pocket factor, whereas the half
18 deprotonated state induces a higher binding affinity, but more importantly, in none of two
19 conditions a decrease in the affinity is observed. This theoretical approach exhibited results
20 that agree qualitatively with the experiments^[45] and represents a useful methodology that,
21 combined with tools for drug design like virtual screening, could be used for designing new
22 biomarkers and optimal strategies for virus-imaging applications.
23
24
25
26
27
28
29
30
31
32
33
34
35
36
37
38
39
40
41
42
43
44
45
46
47

48 **4. Conclusion and Future Perspectives**

49
50 It is clear that atomically precise AuNCs have helped to revolutionize the field of
51 nanomedicine due to their good biocompatibility and extraordinary physicochemical
52 properties. Although the development of AuNCs-based strategies is still in its infancy, their
53 optical features together with low toxicity demonstrated in varied applications, make them
54
55
56
57
58
59
60
61
62
63
64
65

1
2
3
4 promising to overcome challenges like biostability and cytotoxicity that remain pending for
5
6 most of the nanomaterials. Notably, the increasingly detailed knowledge of the structural and
7
8 physicochemical properties provided by the close connection between theoretical and
9
10 experimental studies, offers exciting opportunities for site-specific bio-functionalization of
11
12 the nanoparticle surface. Understanding the details of the internal structure and stability of
13
14 the ligand shell at atomic level, which is particularly well-defined in these systems, allows
15
16 accurate control of the potential surface functional groups. Thus, their precise atomic
17
18 structure provides remarkable advantages for potential applications in drug delivery,
19
20 biomolecule labelling and targeting. Recent advances in force fields will allow exploration
21
22 of the interaction of the engineered AuNCs with the desired environment *via* atomistic
23
24 simulations as well as gaining more insight on the nano–bio interface and protein corona
25
26 complex, which play a pivotal role in the cellular uptake efficiency and biodistribution of the
27
28 nanomaterials throughout the body.
29
30
31
32
33
34
35
36
37

38 Another aspect that needs to be addressed is the high-yield synthesis in order to contribute
39
40 with new affordable strategies compared to conventional methods, as well as the
41
42 improvement of their fluorescence QY with the aim to enhance their use as fluorescence
43
44 imaging agents.
45
46
47
48
49

50 Undoubtedly, further exploration of biocompatible AuNC-based nanosystems must be
51
52 accompanied by theory–experiment investigations for driving this field forward and ideally,
53
54 to achieve their clinical translation in the near future.
55
56
57
58
59
60
61
62
63
64
65

1
2
3
4 **Acknowledgements**
5
6

7 This work was supported by the Academy of Finland (grants 294217, 292352, 319208 and
8 HH's Academy Professorship).
9
10

11
12
13
14
15 **Conflict of Interest**
16

17 The authors declare no conflict of interest.
18
19
20
21
22
23
24

25 **References**
26

- 27
28 [1] S. E. Skrabalak, J. Chen, Y. Sun, X. Lu, L. Au, C. M. Cobley, Y. Xia, *Acc. Chem.*
29 *Res.* **2008**, *41*, 1587.
30
31
32
33 [2] M. Homberger, U. Simon, *Philos. Trans. R. Soc. A Math. Phys. Eng. Sci.* **2010**, *368*,
34 1405.
35
36
37
38 [3] P. Singh, S. Pandit, V. Mokkaapati, A. Garg, V. Ravikumar, I. Mijakovic, *Int. J. Mol.*
39 *Sci.* **2018**, *19*, 1979.
40
41
42
43 [4] Y.-C. Yeh, B. Creran, V. M. Rotello, *Nanoscale* **2012**, *4*, 1871.
44
45
46
47 [5] P. Chhour, P. C. Naha, R. Cheheltani, B. Benardo, S. Mian, D. P. Cormode, in
48 *Nanomater. Pharmacol.*, Springer, **2016**, pp. 87–111.
49
50
51
52 [6] H. Daraee, A. Eatemadi, E. Abbasi, S. Fekri Aval, M. Kouhi, A. Akbarzadeh, *Artif.*
53 *cells, nanomedicine, Biotechnol.* **2016**, *44*, 410.
54
55
56
57 [7] O. B. Adewale, H. Davids, L. Cairncross, S. Roux, *Int. J. Toxicol.* **2019**, *38*, 357.
58
59
60
61
62
63
64
65

- 1
2
3
4 [8] C. M. Goodman, C. D. McCusker, T. Yilmaz, V. M. Rotello, *Bioconjug. Chem.*
5
6 **2004**, *15*, 897.
7
8
9
10 [9] Y. Pan, S. Neuss, A. Leifert, M. Fischler, F. Wen, U. Simon, G. Schmid, W.
11
12 Brandau, W. Jahnen- Dechent, *Small* **2007**, *3*, 1941.
13
14
15 [10] J. F. Hainfeld, D. N. Slatkin, H. M. Smilowitz, *Phys. Med. Biol.* **2004**, *49*, N309.
16
17
18 [11] R. Jin, C. Zeng, M. Zhou, Y. Chen, *Chem. Rev.* **2016**, *116*, 10346.
19
20
21 [12] I. Chakraborty, T. Pradeep, *Chem. Rev.* **2017**, *117*, 8208.
22
23
24 [13] H. Häkkinen, *From gold nanoparticles physics, Chem. Biol.* **2012**, *9*, 233.
25
26
27 [14] T. Tsukuda, H. Häkkinen, *Protected Metal Clusters: From Fundamentals to*
28
29 *Applications*, Elsevier, **2015**.
30
31
32
33 [15] E. Porret, X. Le Guével, J.-L. Coll, *J. Mater. Chem. B* **2020**, *8*, 2216.
34
35
36 [16] N. Kaur, R. N. Aditya, A. Singh, T.-R. Kuo, *Nanoscale Res. Lett.* **2018**, *13*, 302.
37
38
39 [17] Z. Ma, P. Wang, L. Xiong, Y. Pei, *Wiley Interdiscip. Rev. Comput. Mol. Sci.* **2017**, *7*,
40
41 e1315.
42
43
44 [18] H. Häkkinen, *Nat. Chem.* **2012**, *4*, 443.
45
46
47 [19] S. Naahidi, M. Jafari, F. Edalat, K. Raymond, A. Khademhosseini, P. Chen, *J.*
48
49 *Control. release* **2013**, *166*, 182.
50
51
52 [20] X.-D. Zhang, D. Wu, X. Shen, P.-X. Liu, F.-Y. Fan, S.-J. Fan, *Biomaterials* **2012**,
53
54 *33*, 4628.
55
56
57 [21] C. N. Loynachan, A. P. Soleimany, J. S. Dudani, Y. Lin, A. Najer, A. Bekdemir, Q.
58
59
60
61
62
63
64
65

- 1
2
3
4 Chen, S. N. Bhatia, M. M. Stevens, *Nat. Nanotechnol.* **2019**, *14*, 883.
5
6
7 [22] A. K. Iyer, G. Khaled, J. Fang, H. Maeda, *Drug Discov. Today* **2006**, *11*, 812.
8
9
10 [23] R. A. Petros, J. M. DeSimone, *Nat. Rev. Drug Discov.* **2010**, *9*, 615.
11
12
13 [24] M. I. Setyawati, C. Y. Tay, B. H. Bay, D. T. Leong, *ACS Nano* **2017**, *11*, 5020.
14
15
16 [25] K. L. D. M. Weerawardene, E. B. Guidez, C. M. Aikens, *J. Phys. Chem. C* **2017**,
17
18
19
20
21
22
23 [26] H. Yu, B. Rao, W. Jiang, S. Yang, M. Zhu, *Coord. Chem. Rev.* **2019**, *378*, 595.
24
25
26 [27] R. Mout, D. F. Moyano, S. Rana, V. M. Rotello, *Chem. Soc. Rev.* **2012**, *41*, 2539.
27
28
29 [28] C. Auría-Soro, T. Nesma, P. Juanes-Velasco, A. Landeira-Viñuela, H. Fidalgo-
30
31
32
33
34
35
36
37 [29] T.-T. Jia, G. Yang, S.-J. Mo, Z.-Y. Wang, B.-J. Li, W. Ma, Y.-X. Guo, X. Chen, X.
38
39
40
41
42
43
44
45
46
47
48 [30] X. Zhang, Z. Luo, J. Chen, X. Shen, S. Song, Y. Sun, S. Fan, F. Fan, D. T. Leong, J.
49
50
51
52
53
54
55
56
57
58
59 [31] X. Zhang, J. Chen, Z. Luo, D. Wu, X. Shen, S. Song, Y. Sun, P. Liu, J. Zhao, S.
60
61
62
63
64
65
66
67
68
69
70
71
72
73
74
75
76
77
78
79
80
81
82
83
84
85
86
87
88
89
90
91
92
93
94
95
96
97
98
99
100
101
102
103
104
105
106
107
108
109
110
111
112
113
114
115
116
117
118
119
120
121
122
123
124
125
126
127
128
129
130
131
132
133
134
135
136
137
138
139
140
141
142
143
144
145
146
147
148
149
150
151
152
153
154
155
156
157
158
159
160
161
162
163
164
165
- [32] X.-D. Zhang, Z. Luo, J. Chen, S. Song, X. Yuan, X. Shen, H. Wang, Y. Sun, K. Gao,
L. Zhang, *Sci. Rep.* **2015**, *5*, 8669.
- [33] D. Luo, X. Wang, S. Zeng, G. Ramamurthy, C. Burda, J. P. Babilion, *Small* **2019**,

- 1
2
3
4 15, 1900968.
5
6
7 [34] Y. Yang, S. Wang, S. Chen, Y. Shen, M. Zhu, *Chem. Commun.* **2018**, 54, 9222.
8
9
10 [35] L. Milane, M. Trivedi, A. Singh, M. Talekar, M. Amiji, *J. Control. release* **2015**,
11
12 207, 40.
13
14
15 [36] E. Peterson, P. Kaur, *Front. Microbiol.* **2018**, 9, 2928.
16
17
18 [37] P. V Baptista, M. P. McCusker, A. Carvalho, D. A. Ferreira, N. M. Mohan, M.
19
20 Martins, A. R. Fernandes, *Front. Microbiol.* **2018**, 9, 1441.
21
22
23 [38] N.-Y. Lee, P.-R. Hsueh, W.-C. Ko, *Front. Pharmacol.* **2019**, 10, 1153.
24
25
26 [39] K. Zheng, M. I. Setyawati, D. T. Leong, J. Xie, *ACS Nano* **2017**, 11, 6904.
27
28
29 [40] B. Hammer, J. K. Norskov, *Nature* **1995**, 376, 238.
30
31
32 [41] N. Lewinski, V. Colvin, R. Drezek, *small* **2008**, 4, 26.
33
34
35 [42] J. Tang, H. Shi, G. Ma, L. Luo, Z. Tang, *Front. Bioeng. Biotechnol.* **2020**, 8, 1019.
36
37
38 [43] L. P. Silva, A. P. Silveira, C. C. Bonatto, I. G. Reis, P. V Milreu, in *Nanostructures*
39
40 *Antimicrob. Ther.*, Elsevier, **2017**, pp. 577–596.
41
42
43 [44] V. Marjomäki, T. Lahtinen, M. Martikainen, J. Koivisto, S. Malola, K. Salorinne, M.
44
45 Pettersson, H. Häkkinen, *Proc. Natl. Acad. Sci.* **2014**, 111, 1277.
46
47
48 [45] M. Martikainen, K. Salorinne, T. Lahtinen, S. Malola, P. Permi, H. Häkkinen, V.
49
50 Marjomäki, *Nanoscale* **2015**, 7, 17457.
51
52
53 [46] Y. Yang, L. Wang, B. Wan, Y. Gu, *Front. Bioeng. Biotechnol.* **2019**, 7, 320.
54
55
56 [47] M. Azubel, S. D. Carter, J. Weiszmann, J. Zhang, G. J. Jensen, Y. Li, R. D.
57
58
59
60
61
62
63
64
65

- 1
2
3
4 Kornberg, *Elife* **2019**, *8*, e43146.
5
6
7 [48] L. Shang, S. Dong, G. U. Nienhaus, *Nano Today* **2011**, *6*, 401.
8
9
10 [49] H. Liu, G. Hong, Z. Luo, J. Chen, J. Chang, M. Gong, H. He, J. Yang, X. Yuan, L.
11 Li, *Adv. Mater.* **2019**, *31*, 1901015.
12
13
14
15 [50] Y. Liu, J. Li, M. Chen, X. Chen, N. Zheng, *Theranostics* **2020**, *10*, 10057.
16
17
18
19 [51] L. Nie, M. Chen, X. Sun, P. Rong, N. Zheng, X. Chen, *Nanoscale* **2014**, *6*, 1271.
20
21
22 [52] K. L. D. M. Weerawardene, H. Häkkinen, C. M. Aikens, *Annu. Rev. Phys. Chem.*
23 **2018**, *69*.
24
25
26
27 [53] S. Malola, H. Häkkinen, *J. Am. Chem. Soc.* **2019**, *141*, 6006.
28
29
30
31 [54] M. F. Matus, S. Malola, E. K. Bonilla, B. Barngrover, C. M. Aikens, H. Häkkinen,
32 *Chem. Commun.* **2020**, *56*, 8087.
33
34
35
36 [55] E. Pohjolainen, X. Chen, S. Malola, G. Groenhof, H. Häkkinen, *J. Chem. Theory*
37 *Comput.* **2016**, *12*, 1342.
38
39
40
41
42 [56] M. J. Hostetler, A. C. Templeton, R. W. Murray, *Langmuir* **1999**, *15*, 3782.
43
44
45 [57] R. Guo, Y. Song, G. Wang, R. W. Murray, *J. Am. Chem. Soc.* **2005**, *127*, 2752.
46
47
48 [58] M. Montalti, L. Prodi, N. Zaccheroni, R. Baxter, G. Teobaldi, F. Zerbetto, *Langmuir*
49 **2003**, *19*, 5172.
50
51
52
53 [59] C. L. Heinecke, T. W. Ni, S. Malola, V. Mäkinen, O. A. Wong, H. Häkkinen, C. J.
54 Ackerson, *J. Am. Chem. Soc.* **2012**, *134*, 13316.
55
56
57
58
59 [60] V. Rojas-Cervellera, L. Raich, J. Akola, C. Rovira, *Nanoscale* **2017**, *9*, 3121.
60
61
62
63
64
65

- 1
2
3
4 [61] C. J. Ackerson, P. D. Jadzinsky, G. J. Jensen, R. D. Kornberg, *J. Am. Chem. Soc.*
5
6 **2006**, *128*, 2635.
7
8
9
10 [62] K. Salorinne, S. Malola, O. A. Wong, C. D. Rithner, X. Chen, C. J. Ackerson, H.
11
12 Häkkinen, *Nat. Commun.* **2016**, *7*, 1.
13
14
15 [63] P. D. Jadzinsky, G. Calero, C. J. Ackerson, D. A. Bushnell, R. D. Kornberg, *Science*
16
17 (*80-*). **2007**, *318*, 430.
18
19
20
21 [64] T.-R. Tero, S. Malola, B. Koncz, E. Pohjolainen, S. Lautala, S. Mustalahti, P. Permi,
22
23 G. Groenhof, M. Pettersson, H. Häkkinen, *ACS Nano* **2017**, *11*, 11872.
24
25
26 [65] M. Azubel, R. D. Kornberg, *Nano Lett.* **2016**, *16*, 3348.
27
28
29 [66] M. Azubel, A. L. Koh, K. Koyasu, T. Tsukuda, R. D. Kornberg, *ACS Nano* **2017**, *11*,
30
31 11866.
32
33
34
35 [67] E. Pohjolainen, S. Malola, G. Groenhof, H. Häkkinen, *Bioconjug. Chem.* **2017**, *28*,
36
37 2327.
38
39
40
41
42
43
44
45
46
47
48
49
50
51
52
53
54
55
56
57
58
59
60
61
62
63
64
65

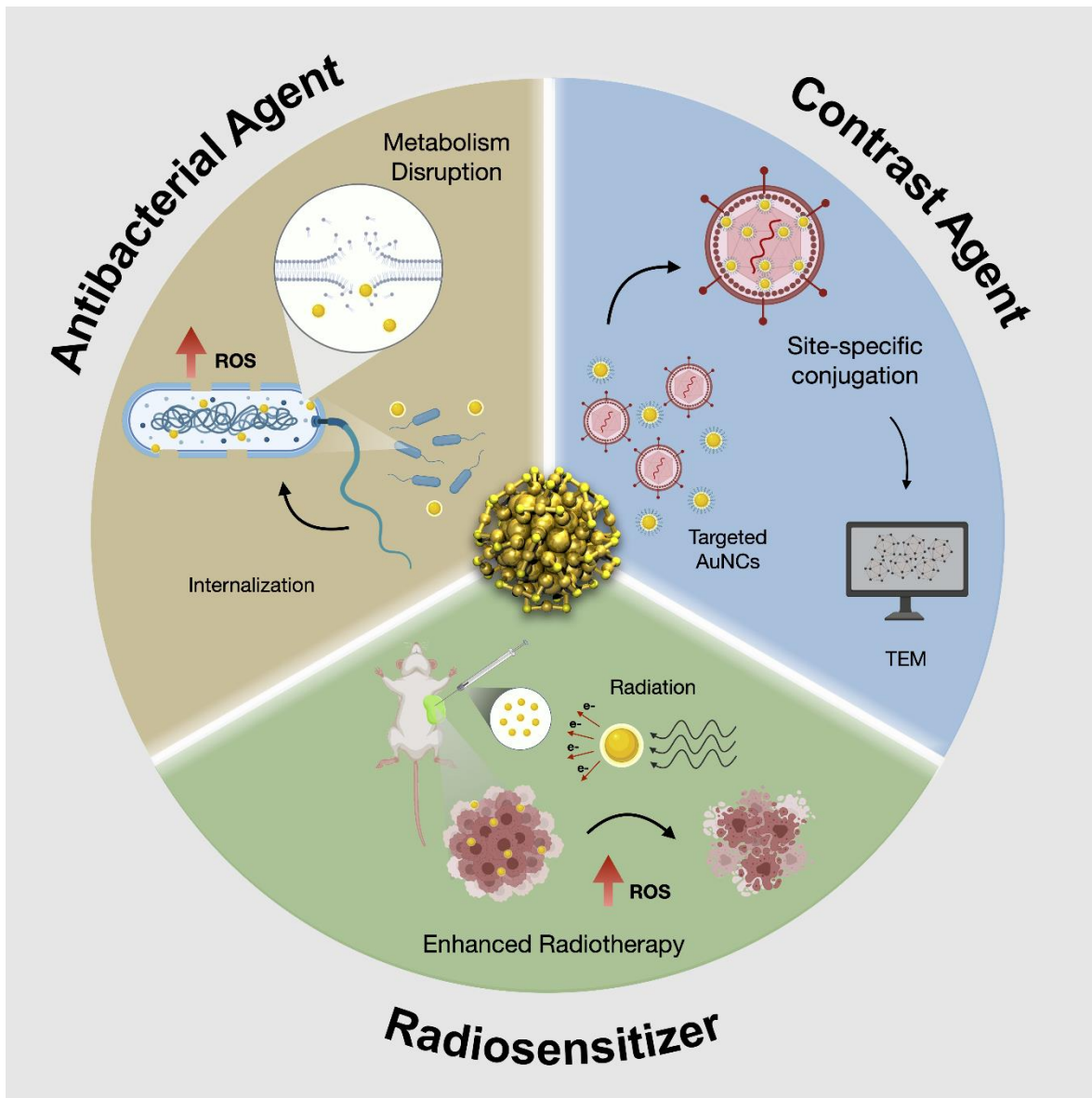


Figure 1. Representative examples of biomedical applications reported by atomically-precise AuNCs: Antimicrobial applications, biological imaging, and radiation therapy. ROS: Reactive Oxygen Species; TEM: Transmission Electron Microscopy.

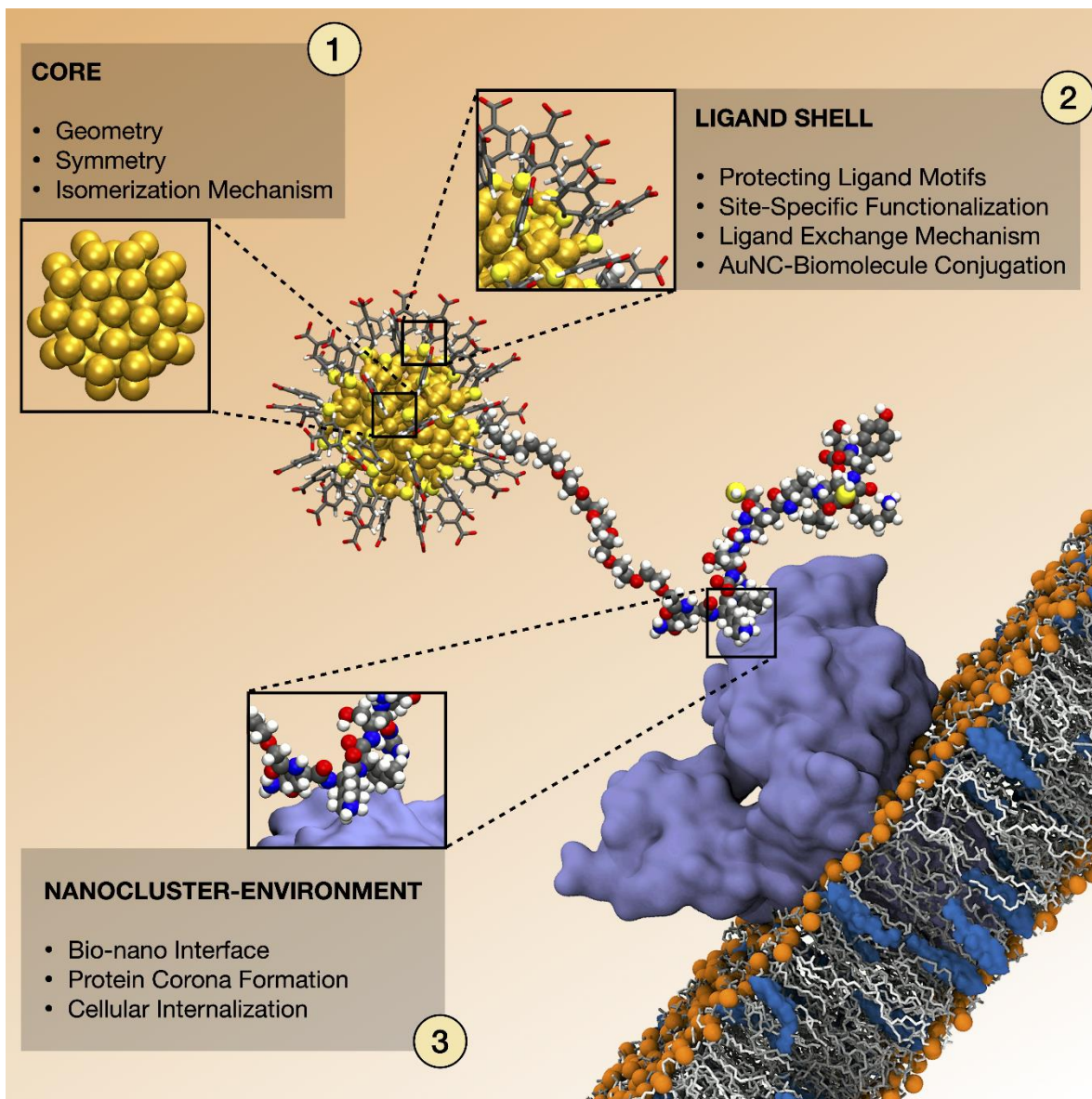
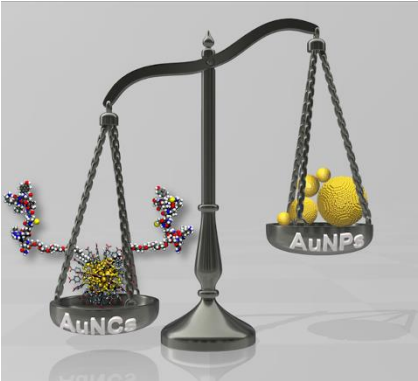


Figure 2. Schematic illustration showing the main aspects that can be precisely explored in the design of biocompatible gold nanoclusters (AuNCs)-based systems by employing a theoretical–experimental approach. A partially exchanged $\text{Au}_{102}(\text{pMBA})_{43}(\text{peptide})_1$ nanocluster is depicted near a typical bilayer of phospholipids. Different physicochemical properties of AuNCs can be either predicted or revealed by a combination of theory (quantum mechanics or molecular mechanics methods) and experimental studies at three levels: 1) core, 2) ligand shell, and 3) nanocluster-environment interface.

1
2
3
4
5
6
7
8
9
10
11
12
13
14
15
16
17
18
19
20
21
22
23
24
25
26
27
28
29
30
31
32
33
34
35
36
37
38
39
40
41
42
43
44
45
46
47
48
49
50
51
52
53
54
55
56
57
58
59
60
61
62
63
64
65

ToC Figure



Atomically precise gold nanoclusters (AuNCs) have helped revolutionize nanomedicine's field due to their excellent biocompatibility and extraordinary physicochemical properties. They have emerged as promising materials to overcome the current challenges of cytotoxicity and biostability present in colloidal gold nanoparticles. Although this revolution is still in its infancy, theoretical/experimental strategies show that the near future is promising!



18
19
20
21
22
23
24
25
26
27
28
29
30
31
32
33
34
35
36
37
38

Dr. María Francisca Matus is a Postdoctoral Researcher in the Nanoscience Center (NSC) at the University of Jyväskylä (Finland) under the direction of Prof. Dr. Hannu Häkkinen. She received her Ph.D. in Science in 2018 at the University of Talca (Chile), where her work was focused on the study and characterization of polymeric nanoparticles as drug delivery systems for cardiovascular diseases. Her recent research focuses on the design and development of multifunctional gold nanoclusters for targeted cancer therapy through theoretical/experimental strategies.



52
53
54
55
56
57
58
59
60
61
62
63
64
65

Prof. Dr. Hannu Häkkinen is a professor in computational nanoscience at the University of Jyväskylä in Finland and a visiting professor in Xiamen, China. His research interests include electronic, optical, magnetic, chemical and catalytic properties of bare, supported, and ligand-protected metal nanoparticles, electrical conductivity of molecule-metal interfaces in

1
2
3
4
5
6
7
8
9
10
11
12
13
14
15
16
17
18
19
20
21
22
23
24
25
26
27
28
29
30
31
32
33
34
35
36
37
38
39
40
41
42
43
44
45
46
47
48
49
50
51
52
53
54
55
56
57
58
59
60
61
62
63
64
65

nanostructures, and structural and chemical properties of metal nanoparticle / virus hybrids.
He has been working on modeling gold nanoclusters for 20 years. He has published about
250 peer-reviewed articles with over 21000 citations and his h-index is 68 (Web of Science).
In 2018, he was listed as one of the “Highly Cited Researchers” by Clarivate Analytics.